From the equivalent circuit of Fig. 4(b), we can write the expression for normalized admittance, presented to guide I, in terms of equivalent network parameter as follows:

$$\bar{Y}_{in} = \left(1 + \frac{1}{1+\bar{X}_{zT}^2}\right) + \frac{j\bar{X}_{zT}}{1+\bar{X}_{zT}^2}. \quad (20)$$

Fig. 8 shows the variation of real and imaginary parts of input admittance as a function of slot length computed from (20) using (16) for $\lambda = 3.2$ cm and slot displacement from center = 2 mm.

## VI. Conclusion

Theoretical results for coupling, input VSWR are in good agreement with the experimental results for the two adjacent waveguides coupled by means of a long narrow slot in the common narrow wall, as well as for the case of *H*-plane Tee junction. The present theory leading to a closed-form expression for the equivalent circuit parameter for coupling apertures is quite general and can be applied for the analysis of electromagnetic coupling between any two arbitrary guides.

## References


[1] L. Lewin, "Some observations on waveguide coupling through medium sized slots," *Proc. Inst. Elect. Eng.*, vol. 107C, no. 12, pp. 171–178, Sept. 1960.

[2] A. J. Sangster, "Variational method for the analysis of waveguide coupling," *Proc. Inst. Elect. Eng.*, vol. 112, no. 12, pp. 2171–2179, Dec. 1965.

[3] V. M. Pandharipande and B. N. Das, "Coupling of waveguides through large apertures," *IEEE Trans. Microwave Theory Tech.*, vol. MTT-26 p. 209, Mar. 1978.

[4] R. Levy, "Analysis and synthesis of waveguide multiaperture directional couplers," *IEEE Trans. Microwave Theory Tech.*, p. 995, Dec. 1968.

[5] N. Marcuvitz, *Waveguide Handbook*. R. L. ser., vol. 10, New York: McGraw-Hill, 1951, chs. 6 and 7.

[6] S. B. Cohn, "Microwave coupling by large apertures," *Proc. IRE*, vol. 4, pp. 696–699, June 1952.

[7] ——, "Determination of apertures parameters by electrolytic tank measurements," *Proc. IRE*, vol. 39, Nov. 1951.

[8] I. B. Levinson and P. Sh. Fredberg, "Slot couplers of rectangular one mode waveguide equivalent circuits and lumped parameters," *Radio Eng. Electron. Phys.*, vol. III, no. 1, pp. 717–724, 1966.

[9] ——, "Slot couplers of rectangular one mode waveguide-numerical results," *Radio Eng. Electron. Phys.*, no. 6, p. 937, 1966.

[10] R. F. Harrington, *Time Harmonic Electromagnetic fields*. New York: McGraw-Hill, 1961, chs. 3 and 8.

[11] N. Marcuvitz and J. Schwinger, "On the representation of electric and magnetic fields produced by currents and discontinuities in waveguides," *J. Appl. Phys.*, vol. 22, pp. 806–819, June 1951.

[12] G. Marcov, *Antennas*. Moscow, USSR: Progress Pub., 1965, ch. 7, p. 205.

[13] S. M. Prasad and B. N. Das, "Studies on waveguide fed slot antennas," *Proc. Inst. Elect. Eng.*, vol. 120, no. 5, pp. 539–540, May 1973.

[14] V. M. Pandharipande and B. N. Das, "Slot coupled Tee junction in rectangular guide *E*-plane," *IEEE Trans. Microwave Theory Tech.*, pp. 65–69, Jan. 1979.

[15] G. A. Yavastropov and S. A. Tsarapkin, "Investigations of slotted waveguide antennas with identical resonant radiators," *Radio Eng. Electron. Phys.*, vol. II, 1965, p. 1429.


# Numerical Calculation of Electromagnetic Energy Deposition for a Realistic Model of Man

MARK J. HAGMANN, MEMBER, IEEE, OM P. GANDHI, FELLOW, IEEE, AND CARL H. DURNEY, MEMBER, IEEE

***Abstract*—Numerical calculations of absorbed energy deposition have been made for a block model of man that is defined with careful attention given to the biometric and anatomical features of a human being. Calculated post-resonant absorption and distribution of energy deposition through the body have better agreement with experimental results than previous calculations made using less realistic models.**

Manuscript received September 18, 1978; revised April 9, 1979.

The authors are with the Departments of Electrical Engineering and Bioengineering, University of Utah, Salt Lake City, UT 84112.

## I. Introduction

WE HAVE used numerical methods with a realistic model to calculate the deposition of electromagnetic energy in man. A block model of man was chosen to allow maximum freedom in defining both the shape and content of the model. We have used the moment-method solution of the electric-field integral equation with a pulse function basis and delta functions for testing [1], [2]. The

0018-9480/79/0900-0804$00.75 ©1979 IEEE

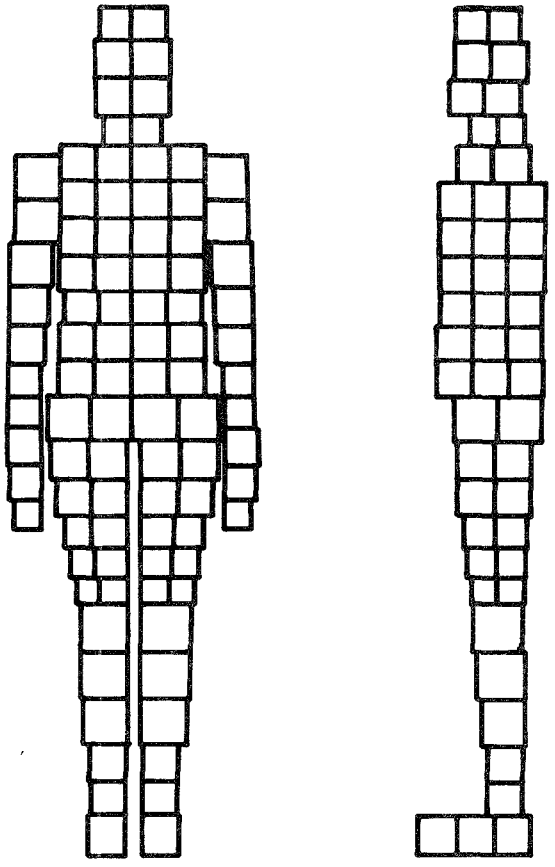

Fig. 1. Improved model of man.

following sections of this paper contain brief descriptions of the improved model and numerical methods, as well as a comparison of the calculations with other numerical and experimental results.

## II. Description of the Model

We have given careful attention to biometric and anatomical diagrams in defining the shape and content of a model having improved realism. A total of 180 cubical cells of various sizes was used to obtain a best fit of the contour on diagrams of the 50th percentile standard man [3]. Sizes and placement of the cells are shown in Fig. 1. Height of the model is 1.75 m.

Partitioning of bone, fat, skin, muscle, lung tissue, air, heart, brain, kidney, liver, and spleen through the cells was done with the aid of anatomical cross sections [4], [5]. Whole-body volume fractions of each tissue type are in agreement with published values. The volume-weighted complex permittivity of each cell was found using properties reported in the literature [6]–[8].

We have forced a plane of symmetry between the left and right body halves in selecting the size, placement, and volume-weighted complex permittivities of the cells. The symmetry has been utilized so that the size of the matrix used in the numerical solutions is determined by 90 cells rather than the total of 180 cells. The symmetry may only be utilized for incident fields in which both $\vec{E}$ and $\vec{k}$ are contained in the plane of symmetry.

## III. Solution of the Matrix Equation

Since one plane of symmetry is used and there are three unknown field components in each cell, the matrix is 270 by 270 complex, which corresponds to a system of 540 simultaneous equations in 540 real unknowns. Solution of the matrix equation is complicated by the matrix being both full and asymmetric. Utilizing symmetry, or cells having different sizes or permittivities, would each be sufficient to destroy symmetry of the matrix.

We have used the successive overrelaxation (SOR) method [9] for iterative solution of the matrix equation. It is known that a matrix having at least one complex eigenvalue, as in the present case, will not allow convergence with SOR unless all eigenvalues have real parts with magnitudes less than unity. Convergence of SOR has the further restriction that the relaxation parameter must be less than a critical value that depends upon the matrix [9]. We have found that convergence with SOR requires a relaxation factor less than unity at 10 MHz, and the critical value decreases with increasing frequency until it reaches zero near 90 MHz. Convergence with SOR is not possible at frequencies exceeding 90 MHz with the present model of man, so we have been forced to use Gauss–Jordan and other noniterative methods [10]. In the present problem when SOR may be used in place of noniterative methods, the computer time is typically reduced by about a factor of four.

We have ordered numbering of cells in the model in such a way that the difference between the numbers for two cells is an increasing function of the distance between the cells. We have formed the matrix using an array of $3 \times 3$ blocks for each cell pair which is inside–out from the structure used previously [11]. The two changes just described have caused the matrix to have a rapid decrease in magnitude of the elements with increasing distance from the diagonal. For all frequencies used so far with the realistic model of man (10–600 MHz), the only matrix elements having appreciable magnitude are contained in a band about the diagonal, which amounts to approximately 10 percent of the entire matrix. The approximation of forced banding may be applied to such a matrix to allow either a large reduction in cost of computations or a significant increase in number of cells [12]. We have not yet implemented forced banding, but we estimate that the method will allow enough cells so that reliable calculations may be made for a realistic model of man to frequencies as high as 2450 MHz.

## IV. Convergence Considerations

Numerical solutions using a pulse function basis can only be exact if there is no variation of $\vec{E}$ within each cell of the model. Solutions having large differences in calculated energy deposition for adjacent cells must have signi-

ficant variation of $\vec{E}$ within the cells, which suggests lack of convergence. Previously reported solutions for block models of man have a ratio of 239:1 for energy deposition in one pair of adjacent cells at 10 MHz [1]. The arrangement and different sizes of cells in the present model cause the maximal ratio of energy deposition for a pair of adjacent cells to be 8:1 at the same frequency.

If $\Delta$ is the side of a cubical cell and $k$ represents the magnitude of the complex propagation vector within the cell, then substantial variation of the electric field must occur within the cell if $k\Delta > \sqrt{6}$ [13]. Thus the pulse function approximation may not be justified at frequencies above 200 MHz with the new model, suggesting an increasing error at higher frequencies. Volume-weighting of the complex permittivity within each cell may also be unjustified at frequencies above 200 MHz though the results appear reasonable to at least 500 MHz.

A numerical solution using a pulse function basis results in a single value representing $\vec{E}$ within each cell. It is possible to use the $E$ values to calculate $1/2\sigma\vec{E}\cdot\vec{E}^*$ for each cell, and to use a volume average to estimate the specific absorption rate (SAR). Large numbers of cells must be used in order to find accurate values of SAR by such a procedure. For example, our calculations of the SAR of a 12-cm muscle cube at 1 MHz show an error of 37 percent with 8 cells, 26 percent with 27 cells, and 20 percent with 64 cells. The delta functions used for testing enforce the integral equation at the center of each cell so that the calculated $\vec{E}$ values are most representative of the cell centers. Inspection of the solutions suggests that the local values of $\vec{E}$ have appreciably less error than occurs in the SAR.

If there is much variation of $\vec{E}$ within a scattering body, then even if we had exact values of $\vec{E}$ at the cell centers, appreciable error would be expected in the calculated SAR. The $N$, supposedly exact, local values of energy deposition constitute samples of an otherwise unknown population so that if large cell-to-cell variation is present, statistical procedures may be used to calculate confidence limits for values of whole-body or part-body SAR [14]. For man at 80 MHz with $\vec{E} \| \hat{L}$ and $\vec{k}$ front-to-back, the 80-percent confidence limits for whole-body SAR are $\pm 12.2$ percent of the mean for the realistic model of man, and $\pm 14.9$ percent of the mean for calulations reported earlier having somewhat greater cell-to-cell variation [1].

We have found that accuracy is improved by using a three-dimensional interpolant with the $\vec{E}$ values initially calculated for each cell to account for some of the variation of $\vec{E}$ within each cell [15]. Trilinear and triquadratic interpolants have both been used to estimate the variation of $\vec{E}$ between the cell centers. The interpolant is integrated in calculating the SAR. For the 12-cm muscle cube at 1 MHz, the SAR found with 27 cells and the triquadratic interpolant have error comparable with the calculation based on 64 cells without the interpolant. The increase in cost due to use of the interpolant is about 1 percent. All values of energy absorption in this paper have been calculated using interpolants.

## V. Comparison of Calculations with Other Results

Fig. 2 shows the values of whole-body SAR calculated for man in free space with $\vec{E} \| \hat{L}$ and an incident intensity of 1 mW/cm$^2$. Points on Fig. 2 represent the results of numerical solutions for the realistic model of man, both with and without the use of an interpolant. The homogeneous approximation of two-thirds the complex permittivity of muscle was used in all calculations for the figure. It is seen in Fig. 2 that the fractional correction which is made by the interpolant increases at high frequencies where increasing error is expected.

Values of whole-body SAR below resonance in Fig. 2 are typically within 10 percent of values calculated for prolate-spheroidal and ellipsoidal models using the same homogeneous approximation of complex permittivity [16]. Experimental results have shown that the SAR for $E$-polarization is inversely proportional to frequency for frequencies from about 1 to 6 times that of resonance [17], [18]. For small animals, such as the rat, the high value of the resonant frequency allows a reduced magnitude for the relative permittivity of tissue so that post-resonant calculations for prolate-spheroidal models may be made using the extended boundary condition method [16]. Such results show the experimentally observed $1/f$ behavior, but the calculations there cannot be directly applied to man. A $1/f$ dependence of the post-resonant SAR is also expected from antenna theory. The anticipated $1/f$ post-resonant behavior is evident in Fig. 2. Earlier numerical solutions suggested a significantly faster roll off between $f^{-1.3}$ and $f^{-1.4}$ [1].

Fig. 3 also shows the whole-body SAR of man in free space with $\vec{E} \| \hat{L}$ and an incident intensity of 1 mW/cm$^2$. The solid curve in Fig. 3 was obtained by splining the 20 values obtained in numerical solutions for the homogeneous realistic model of man. Points on Fig. 3 represent experimental values obtained for human-shaped figurines filled with saline or biological phantom mixtures [17], [18]. The numerical solutions suggest that the resonant frequency is 77 MHz which is somewhat higher than the value of 68–71 MHz determined experimentally.

An important contribution that can be expected from numerical solutions for a realistic model of man is the distribution of energy deposition through the model. Prolate-spheroidal and ellipsoidal models cannot be expected to provide an accurate description of the distribution of energy deposition since the distribution is strongly dependent upon detailed geometry. When the homogeneous approximation of complex permittivity is used, the distribution of energy deposition in the realistic model of man is in good agreement with that found experimentally for homogeneous models [17], [18]. Table I contains numerical and experimental values for the distribution of energy

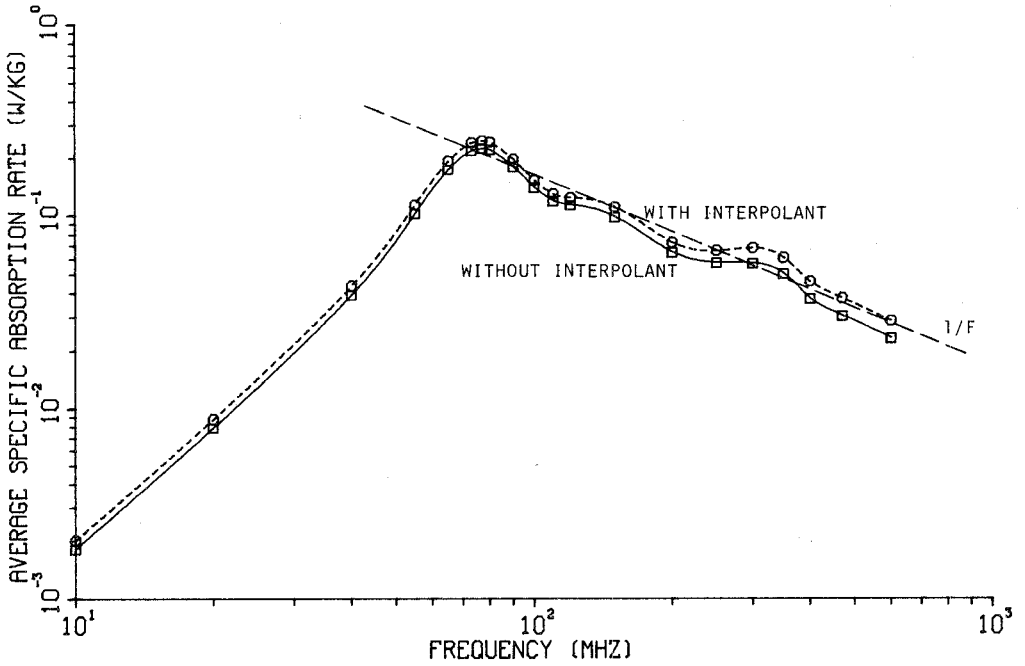


Fig. 2. Whole-body SAR for homogeneous model of man in free space. $\vec{E} \| \hat{L}$, $\vec{k}$ front-to-back, incident intensity = 1 mW/cm$^2$.

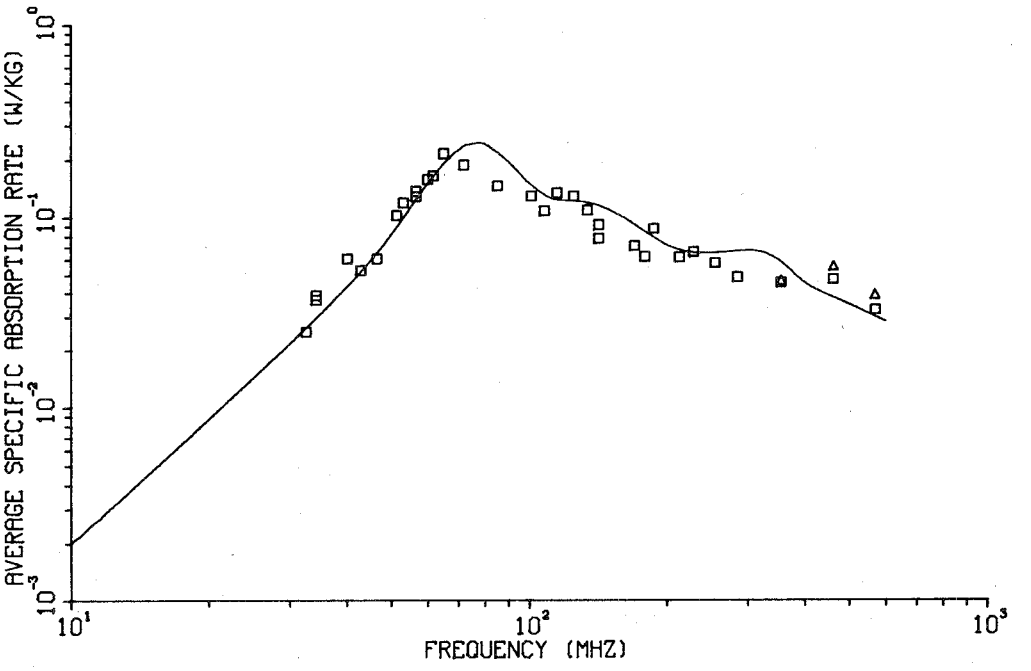


Fig. 3. Whole-body SAR for homogeneous model of man in free space. $\vec{E} \| \hat{L}$, $\vec{k}$ front-to-back, incident intensity = 1 mW/cm$^2$; Squares represent experimental points for saline-filled figurines; Triangles represent experimental values for figurines containing biological phantom mixtures.

TABLE I
DISTRIBUTION OF ENERGY DEPOSITION FOR MAN NEAR RESONANCE IN FREE SPACE[1]

| Body Part | Experimental[2] 68 MHz | Numerical 80 MHz[3] Standard Model | Numerical 80 MHz[3] Thin-Neck Model | Numerical[4] 65 MHz | Numerical[4] 77 MHz |
|---|---|---|---|---|---|
| Eye | 0.043 | 0.0161 | 0.00869 | 0.0415 | 0.0427 |
| Neck | 6.16[5] 3.13 | 0.0717 | 0.137 | 0.286 | 0.318 |
| Heart | 0.415 | 0.131 | 0.104 | 0.251 | 0.327 |
| Pelvic region | 0.154 | 0.192 | 0.211 | 0.171 | 0.233 |
| Thigh | 0.519 | 0.302 | 0.370 | 0.398 | 0.509 |
| Calf | 0.456 | 0.166 | 0.220 | 0.543 | 0.661 |

[1]All values are in units watts per kilogram (W/kg) for incident intensity of 1 mW/cm$^2$; $E \| \hat{L}$, $k$ front-to-back.
[2]Phantom models of man [Gandhi *et al.*, 1975].
[3][Chen *et al.*, 1977].
[4]Calculations for a realistic model of man by the authors.
[5]Commercial dolls used as forms for the phantoms are thought to have exaggerated neck constriction. Neck heating for the dolls is about ten times that of the expected for man.

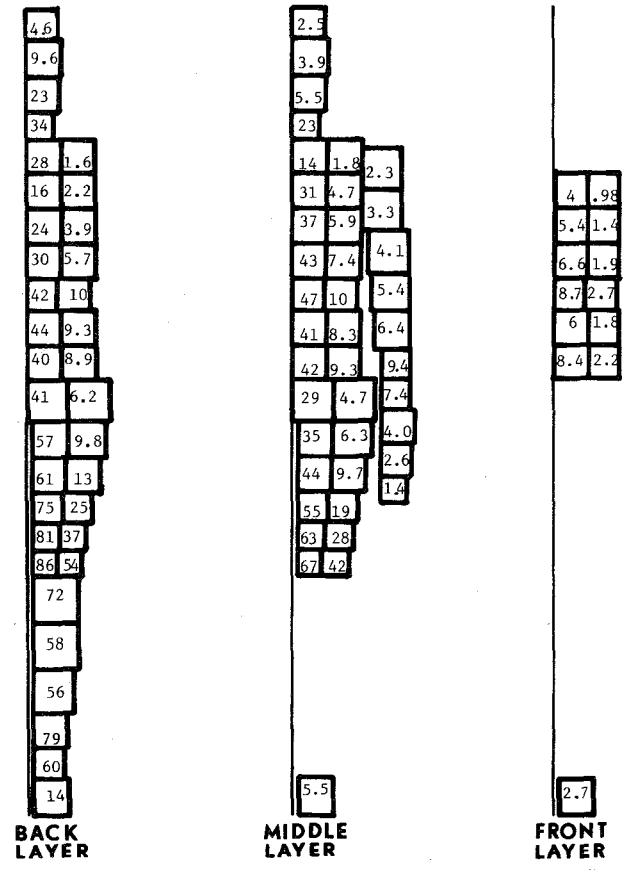


Fig. 4. Local SAR values (watts/kg per mW/cm$^2$)×100 for homogeneous model of man with vertical polarization at 80 MHz.

deposition for man near resonance in free space. The deposition of energy in the regions of the eye, heart, thigh, and calf has been severely underestimated in previous calculations made with less realistic models [1], [11].

When the inhomogeneous complex permittivities are used with the model, a change of less than 2 percent typically occurs in the whole-body average SAR, but the distribution of energy depostition is changed. Figs. 4 and

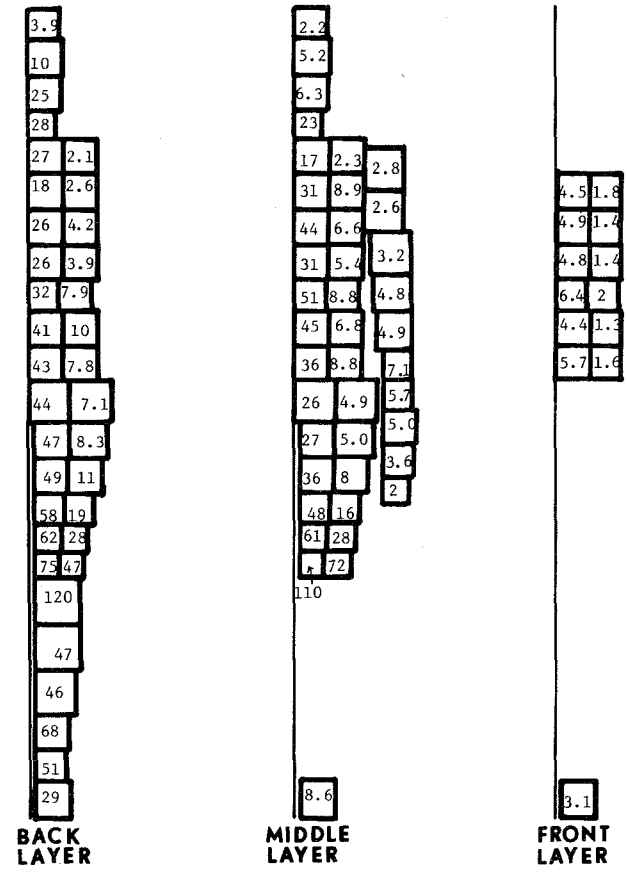


Fig. 5. Local SAR values (watts/kg per mW/cm$^2$)×100 for inhomogeneous model of man with vertical polarization at 80 MHz.

5 illustrate the distribution of absorbed energy in man at 80 MHz in free space for the homogeneous and inhomogeneous models, respectively. One difference is that the inhomogeneous model has reduced absorption in regions with high bone content. Earlier workers have not reported results for inhomogeneous models having a cell-by-cell representation of the dielectric properties.

## VI. CONCLUSIONS

Numerical calculations of absorbed energy deposition have been made for a model of man that has been made with careful attention to both biometric and anatomical diagrams. A total of 180 cells was used in the model, which is a relatively large number for numerical solutions but facilitates accurate modeling.

Calculated post-resonant absorption and distribution of energy deposition through the body have been found to have better agreement with experimental results than previous calculations made using less realistic models.

## ACKNOWLEDGMENT

The authors wish to thank Dr. G. W. Hohmann of the Department of Geology and Geophysics at the University of Utah, Salt Lake City, for use of his computer program which was the starting point for the numerical methods used in the current work.

## REFERENCES

[1] K. M. Chen and B. S. Guru, "Induced EM field and absorbed power density inside human torsos by 1 to 500 MHz EM waves", Tech. Rep. no. 1, under NSF Grant ENG 74-12603, 1976.

[2] G. W. Hohmann, "Three-dimensional polarization and electromagnetic modeling, " *Geophys.*, vol. 40, pp. 309–324, 1975.

[3] N. Diffrient, A. R. Tilley, and J. C. Bardagjy, *Humanscale 1/2/3.* Cambridge, MA: M.I.T. Press, 1974.

[4] D. J. Morton, *Manual of Human Cross Section Anatomy.* (2nd edition), Baltimore, MD: Williams and Wilkins, 1944.

[5] A. C. Eycleshymer and D. M. Schoemaker, *A Cross-Section Anatomy.* New York: D. Appleton, 1911.

[6] C. C. Johnson and A. W. Guy, "Nonionizing electromagnetic wave effects in biological materials and systems," *Proc. IEEE*, vol. 60, pp. 692–718, 1972.

[7] C. C. Johnson, C. H. Durney, and H. Massoudi, "Long wavelength electromagnetic power absorption in prolate spheroidal models of man and animals," *IEEE Trans. Microwave Theory Tech.* vol. MTT-23, pp. 739–747, 1975.

[8] H. P. Schwan, "Electrical properties of tissue and cell suspensions," in *Advances in Biological and Medical Physics.* vol. V, J. H. Lawrence and C. A. Tobias, Eds., New York: Academic Press, 1957, pp. 147–209.

[9] D. M. Young, *Iterative Solution of Large Linear Systems.* New York: Academic, 1971.

[10] B. Carnahan, H. A. Luther, and J. O. Wilkes, *Applied Numerical Methods.* New York: Wiley, 1969.

[11] K. M. Chen and B. S. Guru, "Internal EM field and absorbed power density in human torsos induced by 1–500 MHz EM waves," *IEEE Trans. Microwave Theory Tech.*, vol. MTT-25, pp. 746–756, 1977.

[12] A. J. Poggio and E. K. Miller, "Integral equation solutions of three-dimensional scattering problems," in *Computer Techniques for Electromagnetics.* R. Mittra, Ed., New York: Pergamon, 1973, pp. 159–264.

[13] M. J. Hagmann, O. P. Gandhi, and C. H. Durney, "Upper bound on cell size for moment-method solutions," *IEEE Trans. Microwave Theory Tech.*, vol. MTT-25, pp. 831–832, 1977.

[14] W. Mendenhall and R. L. Scheaffer, *Mathematical Statistics with Applications.* North Scituate, MA: Duxbury, 1973.

[15] M. J. Hagmann, O. P. Gandhi, and C. H. Durney, "Improvement of convergence in moment-method solutions by the use of interpolants," *IEEE Trans. Microwave Theory Tech.*, vol. MTT-26, pp. 904–908, 1978.

[16] C. C. Johsnon, C. H. Durney, P. W. Barber, H. Massoudi, S. J. Allen, and J. C. Mitchell, "Radiofrequency radiation dosimetry Handbook," USAF Rep. SAM-TR-76-35, 1976.

[17] O. P. Gandhi, K. Sedigh, G. S. Beck, and E. L. Hunt, "Distribution of electromagnetic energy deposition in models of man with frequencies near resonance," in *Biological Effects of Electromagnetic waves*, selected papers of the USNC/URSI annual meeting, Boulder, CO, Oct. 20–23, 1975, vol. II, C. C. Johnson and M. L. Shore, eds.; HEW Publication (FDA) 77-8011, U.S. Government Printing Office, Washington, DC 20402.

[18] O. P. Gandhi, E. L. Hunt, and J. A. D'Andrea, "Electromagnetic power deposition in man and animals with and without ground and reflector effects," *Radio Sci.*, vol. 12, no. 6(S), pp. 39–47, 1977.


# Head Resonance: Numerical Solutions and Experimental Results

MARK J. HAGMANN, MEMBER, IEEE, OM P. GANDHI, FELLOW, IEEE, JOHN A. D' ANDREA, AND INDIRA CHATTERJEE, STUDENT MEMBER, IEEE

*Abstract*—**We have used numerical solutions and experiments with phantom models of man, and experiments with the Long Evans rat to show the existence of head resonance. Greatest absorption in the head region of man occurs at a frequency of about 375 MHz. Absorption is stronger for wave propagation from head to toe than it is when the electric field is parallel to the long axis. The highest absorption cross section for the human head is projected to be approximately 3.5 times its physical cross section.**

## I. INTRODUCTION

WE HAVE previously reported numerical solutions for the deposition of electromagnetic energy in a realistic model of man which showed the existence of resonances for body parts such as the head and arms, as well as for the whole body [1]. Further work has been done regarding head resonance, since we believe the phenomenon may be important in the study of behavioral effects, blood-brain barrier permeability, cataractogenesis, and other microwave bioeffects.

Our results show that the first resonance of the intact human head occurs at a frequency of about 375 MHz and has an $S$ parameter (ratio of absorption cross section to physical cross section) of about 3.5 for incident plane waves propagating from head to toe. Earlier calculations for a spherical model of the isolated human head showed a geometrical resonance with $S = 1.1$ near 450 MHz, and a second resonance with $S = 1.4$ occurring near 2.1 GHz when allowance is made for the inhomogeneous structure by using a multilayered model [2]. The results of our study

Manuscript received October 16, 1978; revised February 23, 1979.

The authors are with the Departments of Electrical Engineering and Bioengineering, University of Utah, Salt Lake City, UT 84112.

0018-9480/79/0900-0809$00.75 ©1979 IEEE